

Reversible color changes of metal(II)-N¹,N³-di(pyridin-4-yl)isophthalamide complexes *via* desolvation and solvation†

Yun Gong,^{a,b} Yuchao Zhou,^b Jinghua Li,^c Rong Cao,^{*a} JianBo Qin^b and Jian Li^b

Received 19th April 2010, Accepted 12th August 2010

DOI: 10.1039/c0dt00326c

Four metal(II)-N¹,N³-di(pyridin-4-yl)isophthalamide (L) complexes formulated as [Cu(L)₂Cl₂].5.5H₂O (1), [Ni(L)₂Cl₂].5.5H₂O (2), [Co(L)(*m*-BDC)].DMF (3) (*m*-BDC = 1, 3-benzenedicarboxylic dianion) and [Cd₂(L)₂(*m*-BDC)₂].DMF.0.2H₂O (4) have been solvothermally synthesized and structurally characterized by single-crystal X-ray diffractions. Complexes 1 and 2 are isomorphous, both of them exhibit chain-like frameworks, in which ligand L shows a *cis*-conformation. Complex 3 displays a three dimensional architecture constructed by ligand L with *intermediate*-conformation linking different chains. Complex 4 shows a corrugated two dimensional layer in which ligand L with *trans*-conformation and *m*-BDC act as bridging groups linking different Cd(II) centers. The four complexes all possess stable host frameworks, and complexes 1–3 show reversible color changes *via* desolvation and solvation.

Introduction

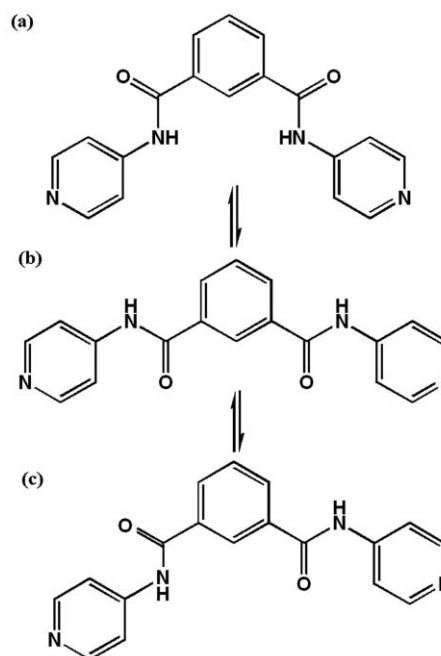
The reversible color or luminescence changes of chromophoric molecules in different solvents is called solvatochromism.^{1–2} Solvatochromism is caused by the change in the energy gap between a ground state and excited state of the compound, which results from the specific interactions between chromophore and solvent molecules. Organic conjugated polymers change their conformations in certain solvents and give rise to a solvatochromic response.^{1f} Some transition metal complexes can undergo solvatochromic changes and these changes often result from the subtle structural changes of the coordination center due to the solvent attack, leading to the energy alteration of the visible d–d transition.²

Solvent indicator plays an important role in many fields. Usually, the preparation of solvent indicator is based on the principle of solvatochromism. However, solvatochromism usually appears in solution and a large amount of solvent is involved, which prevents the improvement of the sensitivity to solvent, and it is not feasible for the recycling of the solvent indicator.³

As analogues of zeolites and clays, metal–organic frameworks (MOFs) containing channels or voids have attracted current interest because of their functional properties and practical applications.^{4–5} Up until now, changes of properties⁶ such as color changes of the stable porous MOFs during desolvation and re-absorption has rarely been investigated.

In this work, we used a flexible bis(pyridyl) ligand, N¹,N³-di(pyridin-4-yl) isophthalamide (L), which possesses different

conformations due to the rotation of the flexible C–N single bonds in the structure. Its three typical conformations are shown in Scheme 1. Based on the flexible ligand and Pt(II), Puddephatt's group has obtained several metallamacrocycles and metallacages.^{7a–d} Dastidar's group has reported the *cis*-conformation of the L ligand in Co(II)–L and Cd(II)–L complexes.^{7e} In the present paper, we obtained two isomorphous 1D porous MOFs: [Cu(L)₂Cl₂].5.5H₂O (1) and [Ni(L)₂Cl₂].5.5H₂O (2). Utilizing the coligand, 1,3-benzenedicarboxylic acid (*m*-H₂BDC), we got two complexes: [Co(L)(*m*-BDC)].DMF (3) and [Cd₂(L)₂(*m*-BDC)₂].DMF.0.2H₂O (4), which exhibit 3D and 2D architectures, respectively. In complexes 1 and 2, ligand L shows a *cis*-conformation. In complexes 3 and 4, L displays an *intermediate*- and a *trans*-conformation, respectively. The four



Scheme 1 The *cis*- (a), *intermediate*- (b) and *trans*- (c) conformations of the ligand L.

^aState Key Laboratory of Structural Chemistry, Fujian Institute of Research on the Structure of Matter, Chinese Academy of Sciences, Fuzhou, Fujian 350002, P. R. China. E-mail: rcao@fjirsm.ac.cn; Fax: +86-591-83796710

^bDepartment of Chemistry, College of Chemistry and Chemical Engineering, Chongqing University, Chongqing 400044, P. R. China

^cDepartment of Pharmaceutical Chemistry, College of Chemistry and Chemical Engineering, Chongqing University, Chongqing 400044, P. R. China

† Electronic supplementary information (ESI) available: TGA diagrams, PXRD patterns and colour changes of the compounds. Additional data. CCDC reference numbers 707618 and 771991–771993. For ESI and crystallographic data in CIF or other electronic format see DOI: 10.1039/c0dt00326c

complexes all possess stable host frameworks and complexes **1–3** show reversible color changes *via* desolvation and solvation.

Experimental

Materials and methods

All chemicals purchased were reagent grade and used without further purification. C, H, N elemental analyses were performed on an Elementar Vario EL III analyzer. IR spectra were recorded as KBr pellets on a PerkinElmer spectrometer. TGA was performed on a NETZSCH STA 449C thermogravimetric analyzer in flowing N₂ with a heating rate of 10 °C min⁻¹. The PXRD data were collected on a RIGAKU DMAX2500PC diffractometer using Cu-K α radiation. UV-Vis spectra were measured on a Lambda-900 UV spectro-photometer. All measurements were performed at room temperature.

Synthesis

Synthesis of C₁₈H₁₄N₄O₂. The ligand was prepared according to the literature.⁷ Elemental Anal. Calcd. for C₁₈H₁₄N₄O₂: C, 67.92; H, 4.40; N, 17.61%. Found: C, 68.02; H, 4.50; N, 17.88%. IR (cm⁻¹): 3234(s), 1950(w), 1684(s), 1600(s), 1509(s), 1415(s), 1329(s), 1290(s), 1207(s), 1073(s), 995(s), 828(s), 715(s), 580(m), 539(m).

Synthesis of [Cu(L)₂Cl₂] \cdot 5.5H₂O (1). A mixture of CuCl₂ \cdot 2H₂O (0.5 mmol, 0.085 g), L (0.5 mmol, 0.159 g) and DMF (10 mL) was heated at 120 °C in a Teflon-lined autoclave for 2 days, followed by slow cooling to room temperature. The resulting blue prismatic crystals were filtered off (yield: *ca.* 95% based on L). Elemental Anal. Found: C, 49.35; H, 4.55; N, 13.03%. Calcd. for C₃₆H₃₉N₈O_{9.5}CuCl₂: C, 49.66; H, 4.48; N, 12.87%. IR (cm⁻¹): 3425(s), 1689(m), 1666(s), 1597(s), 1516(s), 1425(m), 1333(s), 1300(s), 1211(s), 1018(m), 841(m), 719(m), 542(m).

Synthesis of [Ni(L)₂Cl₂] \cdot 5.5H₂O (2). The preparation of complex **2** was similar to that of complex **1** except that NiCl₂ \cdot 6H₂O was used instead of CuCl₂ \cdot 2H₂O. The yield of the green prismatic crystals is *ca.* 95% based on L. Elemental Anal. Found: C, 50.15; H, 4.25; N, 13.13%. Calcd. for C₃₆H₃₉N₈O_{9.5}NiCl₂: C, 49.94; H, 4.51; N, 12.95%. IR (cm⁻¹): 3420(s), 1690(m), 1668(s), 1597(s), 1516(s), 1425(m), 1334(s), 1300(s), 1211(s), 1020(m), 843(m), 721(m), 542(m).

Synthesis of [Co(L)(*m*-BDC)] \cdot DMF (3). The synthesis of complex **3** was carried out as described above for complex **1**, but starting with the mixture of Co(NO₃)₂ \cdot 6H₂O (0.05 mmol, 0.015 g), L (0.05 mmol, 0.016 g), *m*-H₂BDC (0.05 mmol, 0.008 g) and DMF (8 mL). Yield: *ca.* 90% based on L. Elemental Anal. Found: C, 56.59; H, 4.02; N, 11.58%. Calcd. for CoC₂₉N₅H₂₅O₇: C, 56.68; H, 4.07; N, 11.40%. IR (cm⁻¹): 3435(s), 1666(s), 1597(s), 1516(s), 1426(m), 1334(s), 1299(s), 1211(s), 1020(m), 843(m), 512(w).

Synthesis of [Cd₂(L)₂(*m*-BDC)₂] \cdot DMF \cdot 0.2H₂O (4). The preparation of complex **4** was similar to that of complex **3** except using CdSO₄ \cdot 8/3H₂O (0.05 mmol, 0.013 g) instead of Co(NO₃)₂ \cdot 6H₂O. Yield: *ca.* 90% based on L. Elemental Anal. Found: C, 52.29; H, 4.23; N, 9.85%. Calcd. for C₅₅N₉H_{43.4}Cd₂O_{13.2}: C, 52.13; H, 4.11; N, 9.95%. IR (cm⁻¹): 3454(s), 1661(s), 1597(s), 1514(s), 1425(m), 1333(m), 1211(s), 1045(w), 831(w), 715(w), 544(m).

X-Ray crystallography†

XRD data of complexes **1–4** were collected on a Bruker-AXS CCD area detector-equipped diffractometer with graphite-monochromatized Mo K α (λ = 0.71073 Å) radiation at room temperature. An empirical absorption correction from ψ scan was applied. All the structures were solved by direct methods and expanded using Fourier techniques. The non-hydrogen atoms were refined anisotropically. All of the hydrogen atoms were placed in the calculated positions. All calculations were performed using the SHELXTL-97 program. The solvent molecules in complexes **1** and **2** were highly disordered and were impossible to refine using conventional discrete-atom models, thus the contribution of partial solvent electron densities were removed by the SQUEEZE routine in PLATON.⁸ The final chemical formula was estimated from the SQUEEZE results combined with the TGA results. Crystal data and structure refinements for complexes **1–4** are listed in Table 1. Further details are provided in the ESI.†

Results and discussion

Synthesis

Complexes **1** and **2** not only can be synthesized solvothermally, but can also be prepared *via* diffusion technique at room temperature. Dissolving MCl₂ (M = Cu²⁺ or Ni²⁺) and L in DMF, the resulting solution was added to a layer of CH₂Cl₂, after several days, crystals suitable for study of X-ray diffraction were obtained. The preparation of the two complexes was not susceptible to molar ratio of reactants. The molar ratio of MCl₂/L can range from 1:1 to 3:1. Complex **1** can be obtained even when CuCl was used instead of CuCl₂ \cdot 2H₂O. Complex **2** can selectively crystallize from a mixture of L, NiCl₂ \cdot 6H₂O and NiSO₄ \cdot 6H₂O. It is indicated that complexes **1** and **2** are thermally stable compounds under the reaction condition.

Complexes **3** and **4** were obtained under similar conditions except different metal salts were utilized. Their different structures indicate the species of metal salts plays an important role in the syntheses of coordination polymers.

Crystal structures and thermal stability

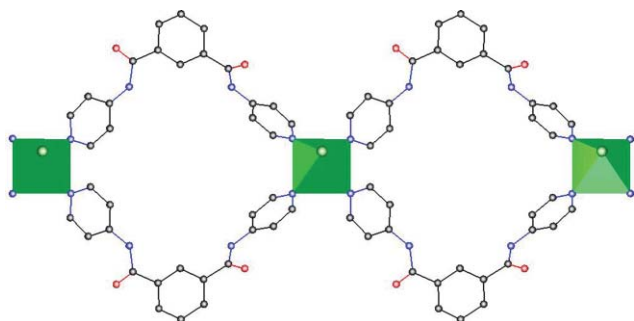
Crystal structures and thermal stability of [Cu(L)₂Cl₂] \cdot 5.5H₂O (1) and [Ni(L)₂Cl₂] \cdot 5.5H₂O (2). Single-crystal X-ray diffraction analyses reveal that complexes **1** and **2** are isomorphous (Table 1). Therefore, we will restrict our description to the copper complex **1** and only mention pertinent points for the nickel complex **2** where appropriate.

Complex **1** crystallizes in the trigonal space group *P*3₁2₁ (no. 152), whereas complex **2** crystallizes in the trigonal space group *P*3₂2₁ (no. 154). The Flack parameters of the two complexes are zero, indicating they possess opposite absolute structures.

In the copper complex **1**, the asymmetric unit contains half Cu(II), one L, one Cl⁻, one fourth dissociated water molecules. The Cu(II) center is coordinated by four nitrogen atoms from four L [Cu–N 2.029(4)–2.030(4) Å, N–Cu–N 89.0(2)–177.1(2)°] and two Cl⁻ to furnish an octahedral geometry [Cu–Cl 2.848 Å] (Fig. 1). In the nickel complex **2**, the Ni–N bond lengths range from 2.103(4) to 2.106(4) Å, the N–Ni–N bond angles are in the range of 88.9(2)–177.4(2)°, and the Ni–Cl bond length is 2.490(1) Å.

Table 1 Crystal data and structure refinements for complexes 1–4

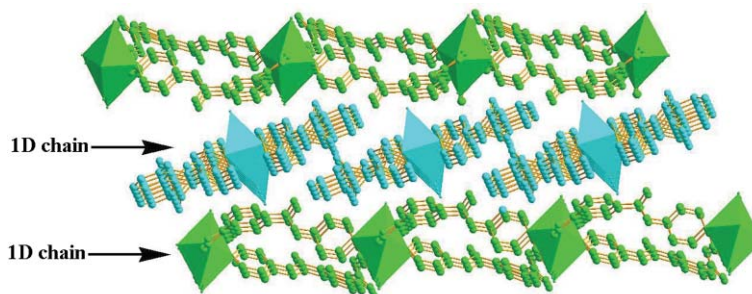
Complex	1	2	3	4
Empirical formula	C ₃₆ H ₃₉ N ₈ O _{9.5} CuCl ₂	C ₃₆ H ₃₉ N ₈ O _{9.5} NiCl ₂	CoC ₂₉ N ₅ H ₂₅ O ₇	C ₅₅ N ₉ H _{43.4} Cd ₂ O _{13.2}
<i>M</i>	870.33	865.33	614.47	1266.42
Crystal system	Trigonal	Trigonal	Mono-clinic	Mono-clinic
Space group	<i>P</i> 3 ₁ 2 ₁	<i>P</i> 3 ₁ 2 ₁	<i>C</i> 2/ <i>c</i>	<i>C</i> 2/ <i>c</i>
<i>a</i> /Å	14.3159(4)	14.4083(3)	16.7156(17)	30.151(3)
<i>b</i> /Å	14.3159(4)	14.4083(3)	11.1345(12)	9.9652(5)
<i>c</i> /Å	19.4452(11)	18.9964(8)	32.121(3)	19.3515(16)
α /°	90	90	90	90
β /°	90	90	91.554(2)	109.463(4)
γ /°	120	120	90	90
<i>V</i> /Å ³	3451.3(2)	3415.29(18)	5976.2(10)	5482.1(7)
<i>Z</i>	3	3	8	4
<i>D_c</i> /Mg m ⁻³	1.125	1.129	1.366	1.525
μ /mm ⁻¹	0.632	0.585	0.627	0.848
θ range/°	2.66 to 27.48	2.70 to 27.46	2.28 to 25.01	2.21 to 25.01
Range <i>hkl</i>	–18 to 18 –18 to 18 –25 to 25	–18 to 18 –18 to 18 –24 to 24	–12 to 19 –11 to 13 –36 to 38	–35 to 35 –11 to 11 –23 to 19
Refins collected	26 740	26 820	15 256	16 888
Unique refins	5280	5208	5210	4813
No. of parameters	237	241	421	380
<i>F</i> (000)	1197	1194	2536	2522
<i>R</i> ₁	0.0793	0.0776	0.0640	0.0535
w <i>R</i> ₂ [<i>I</i> > 2σ(<i>I</i>)]	0.2202	0.2266	0.1555	0.1396
<i>R</i> ₁	0.0895	0.0851	0.1111	0.0699
w <i>R</i> ₂ [all data]	0.2304	0.2370	0.1767	0.1676
GOF	1.068	1.112	0.963	1.227

**Fig. 1** 1D porous framework of complex 1 (C, N, O atoms and {CuN₄Cl₂} octahedra are black, blue, red and green, respectively, H atoms and water molecules are omitted for clarity).

In complex 1, the crystallographically unique ligand L exhibits a *cis*-conformation (Scheme 1(a) and Fig. 1). The dihedral angles between its phenyl ring and two pyridine rings are 41.5 and 40.9°,

respectively. Two deviated L ligands form a cavity and different Cu(II) centers are connected by two strands of L ligands to form a 1D porous framework with a Cu...Cu separation of 14.316 Å. The size of the cavity is *ca.* 9.0 Å × 9.9 Å.

Different 1D chains are not stacked parallel, but in a staggered mode to form a 3D supramolecular network (Fig. 2). Strong H bond interactions between chains are observed in complex 1. For example: H4–N4: 0.86 Å, H4...Cl1A: 2.38 Å, N4...Cl1A: 3.20 Å, ∠N4–H4...Cl1A: 157.9° (atom with additional label A refers to the symmetry operations: *y* – 1, *x*, –*z* + 2). Due to the molecular stacking, the solvent-accessible volume of the unit cell of complex 1 was estimated to be 1212.7 Å³, which is approximately 35.1% of the unit-cell volume (3451.3(7) Å³) (PLATON program⁹). Strong H bond interactions also exist between solvent water and 1D chains, for example: H3–N3: 0.86 Å, H3...OWB: 2.06 Å, N3...OWB: 2.88 Å, ∠N3–H3...OWB: 159.9° (atom with additional label B refers to the symmetry operations: *y*, *x*, –*z* + 1).

**Fig. 2** 1D chains are stacked in a staggered mode to form a 3D supramolecular network in complex 1 (H atoms and water molecules are omitted for clarity).

In complex **2**, the corresponding dihedral angles are 37.6 and 37.7°, respectively. The Ni...Ni separation is 14.408 Å and the size of the cavity is *ca.* 9.2 × 9.7 Å. The solvent-accessible volume of the unit cell of complex **2** was estimated to be 1174.4 Å³, which is approximately 34.4% of the unit-cell volume (3415.3 Å³) (PLATON program⁹). Strong H bonds are also observed not only between chains, but also between water and 1D chains in complex **2**. For example: H4–N4: 0.86 Å, H4...Cl1C: 2.45 Å, N4...Cl1C: 3.26 Å, ∠N4–H4...Cl1C: 157.6°; H2–N2: 0.86 Å, H2...O3: 2.11 Å, N2...O3: 2.92 Å, ∠N2–H2...O3: 157.3° (atom with additional label C refers to the symmetry operations: *y*, *x*, *-z*).

Thermogravimetric analyses (TGA) were carried out to examine the thermal stability of the two complexes (Fig. S1, ESI†). The samples were heated up to 1000 °C in N₂.

It is found that the cavities of complexes **1** and **2** are occupied by 5.5 solvent water molecules per unit, as estimated by SQUEEZE and TGA. The TGA curves of both complexes **1** and **2** show a one step weight loss of 11.4% between 30 and 210 °C corresponding to the loss of the water molecules (calc. 11.4 wt%) in the cavities (Fig. S1(a) and (b), ESI†). The number of the water molecules and the TG results are in agreement with the data for the isomorphous Co(II)–L complex in previous work.^{7e} Strong H bonds between the solvent molecules and the host frameworks as well as the small voids resulted from the staggered 1D chains in the structures of complexes **1** and **2** can prevent solvent molecules to be easily lost.

As for complexes **1** and **2**, the dehydrate MOFs remain stable up to ~310 °C without any weight loss (Fig. S1(a) and (b), ESI†), showing that 1D frameworks could retain structural integrity to *ca.* 310 °C. It is evidenced by the powder XRD patterns of the products, which are in good accordance with the simulated powder XRD patterns of complexes **1** and **2** (Fig. S2(a) and (b), ESI†). It can be concluded that complexes **1** and **2** has excellent thermal stability in the class of MOFs.^{4–5} The high stability of the porous 1D MOFs may be attributed to the L-bridged double chains and strong H bonds between chains.

Crystal structure and thermal stability of [Co(L)(*m*-BDC)]·DMF (3). Complex **3** crystallizes in *C2/c* space group, its asymmetric unit contains one crystallographically unique Co(II) ion, one unique L ligand, one unique *m*-BDC and two unique half dissociated DMF molecules. There are two crystallographically unique carboxylate groups, one of them exhibits a chelating coordination mode, and the other shows a bis-monodentate coordination mode to link two Co(II) centers (Fig. 3).

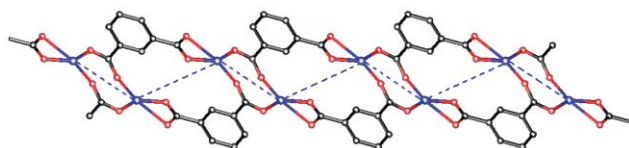


Fig. 3 1D chain linked by *m*-BDC in complex **3** with the Co...Co separation indicated by dashed lines (H atoms, solvent DMF and ligand L omitted for clarity).

Each Co(II) ion is six-coordinated by four O atoms from three carboxylate groups of three *m*-BDC and two N atoms from two L ligands to furnish a distorted octahedral geometry. The Co–O bond lengths range from 2.006(4) to 2.349(4) Å and the

O–Co–O bond angles range from 58.9(1) to 160.3(1)°. The two N atoms from L ligands occupy the axial positions of {CoO₄N₂} octahedron and the equatorial positions are occupied by the four carboxylate O atoms. Two of the O atoms are from the chelating carboxylate group and the other two are from two bis-monodentate carboxylate groups (Fig. 3). Different Co(II) centers are linked by two strands of *m*-BDC to form a chain with an alternating Co...Co separation of 4.421 and 7.029 Å (Fig. 3).

As shown in Fig. 4, the 1D chains run through several directions. L ligand links different chains and complex **3** exhibits a 3D architecture. In complex **3**, L shows an *intermediate*-conformation (Scheme 1(b) and Fig. 4) and the dihedral angles between the phenyl ring and two pyridine rings are 45.0 and 34.7°, respectively (Fig. 4). According to PLATON program,⁹ the solvent-accessible volume of the unit cell of complex **3** was estimated to be 1824.9 Å³, which is approximately 30.5% of the unit-cell volume (5976.2 Å³). Strong H bonds are observed not only within the 3D architecture, but also between solvent DMF and the 3D architecture. For example, H1–N1: 0.86 Å, H1...O1D: 2.10 Å, N1...O1D: 2.92 Å, ∠N1–H1...O1D: 160.0°; H3–N3: 0.86 Å, H3...O8: 2.09 Å, N3...O8: 2.82 Å, ∠N3–H3...O8: 143.4° (atom with additional label D refer to the symmetry operations: D *-x* + 1, *-y* + 2, *-z* + 1).

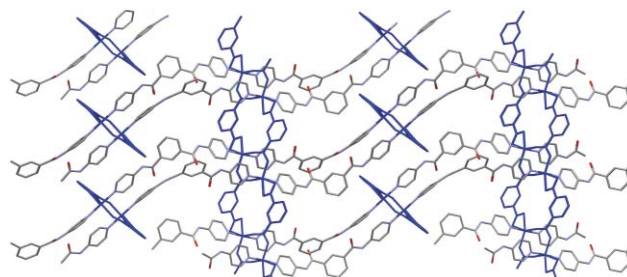


Fig. 4 1D chains in several directions (denoted in blue) linked by L ligands to construct a 3D architecture in complex **3** (H atoms and solvent DMF omitted for clarity).

As shown in Fig. S1(c), ESI,† complex **3** loses its solvent DMF molecules in the range from 150 to 250 °C with a loss of 12.0 wt% (calc. 11.9 wt%). The desolvated MOF doesn't lose weight up to ~350 °C. The PXRD pattern of the desolvated sample is in good accordance with the simulated PXRD pattern of complex **3** (Fig. S2(c), ESI†), indicating the porous framework is retained in the absence of guest DMF molecules.

Crystal structure and thermal stability of [Cd₂(L)₂(*m*-BDC)₂]·DMF·0.2H₂O (4). Complex **4** crystallizes in *C2/c* space group, its asymmetric unit contains one Cd(II), one L, one *m*-BDC, half dissociated disordered DMF and one tenth dissociated water molecule.

Cd(II) center in complex **4** exhibits a square pyramidal geometry and is five coordinated by three oxygen atoms from two carboxylate groups of two *m*-BDC and two nitrogen atoms from two L ligands. One of the two carboxylate group exhibits a chelating coordination mode and another shows a monodentate coordination mode with one O atom uncoordinated. The O–Cd–O bond angles range from 54.1(1) to 125.1 (2)°. The N–Cd–N bond angle is 96.8(2)°, indicating the neighboring two L ligands are almost perpendicular to each other. The crystallographically

unique L ligand exhibits a *trans*-conformation (Scheme 1(c) and Fig. 5) and the corresponding dihedral angles are 70.4 and 48.2°, respectively. Therefore complex **4** shows a corrugated 2D layer in which bent L ligand and *m*-BDC act as bridging groups linking different Cd(II) centers (Fig. 5).

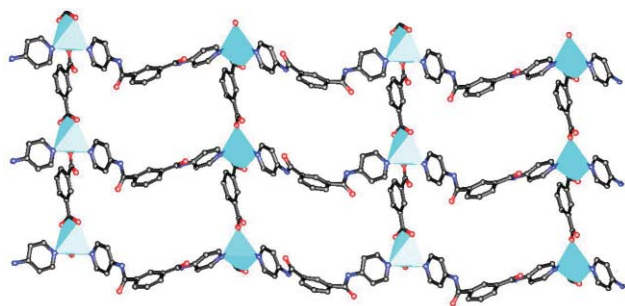


Fig. 5 The corrugated 2D layer of complex **4** (H atoms, dissociated DMF and water omitted for clarity).

Different layers in complex **4** stacked in an AA sequence *via* strong interlayer H-bonds and complex **4** shows a 3D supramolecular architecture (Fig. 6). For example: H2–N2: 0.86 Å, H2...O1E: 2.28 Å, N2...O1E: 3.05 Å, \angle N2–H2...O1E: 149.7°; H4–N4: 0.86 Å, H4...O2F: 2.12 Å, N4...O2F: 2.96 Å, \angle N4–H4...O2F: 163.4° (atom with additional labels E, F refer to the symmetry operations: E– $x + 1/2$, $y - 1/2$, $-z + 3/2$; F– $x + 1/2$, $-y + 3/2$, $-z + 1$). According to PLATON program,⁹ the solvent-accessible volume of the unit cell of complex **4** was estimated to be 1103.5 Å³, which is approximately 20.1% of the unit-cell volume (5482.1 Å³). However, no strong H bond is observed between solvents and the 2D layers.

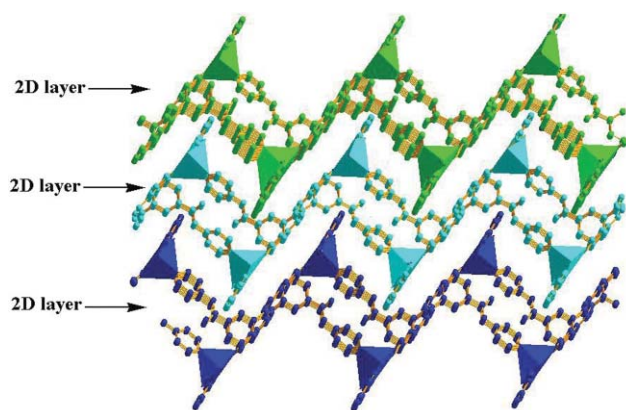


Fig. 6 The AA stacking mode of the wave-like layers in complex **4** (H atoms, solvent DMF and water omitted for clarity).

Complex **4** shows a one step weight loss of 6.1% between 30 and 230 °C corresponding to the loss of the water and DMF molecules (calc. 6.0 wt%) in the structure. The desolvated MOF doesn't lose weight up to ~390 °C. (Fig. S1(d), ESI†). The PXRD pattern of the desolvated MOF in excellent agreement with the simulated PXRD pattern of complex **4** (Fig. S2(d), ESI†), shows it retains the structural integrity up to *ca.* 300 °C.

As described above, complexes **1–4** all possess stable host frameworks. In terms of Kitagawa's classification, they belong to the second generation of porous MOFs.⁵ The structural retention

via desolvation and salvation is probably due to the flexible L ligand in the structure. The flexible C–N single bond can rotate freely to some extent and it is possible not to damage the original framework when solvent molecules in the channel are removed.

Color change and UV-Vis spectra

At room temperature, the color of complexes **1–4** is blue, green, red and white, respectively. After being evacuated at 100 °C in vacuum for 2 h, the color of complexes **1–3** becomes green, off-white and purple, respectively except that the color of complex **4** is unchanged and still white. The PXRD patterns of the evacuated samples are similar from those simulated using the single-crystal data, which indicates that the host frameworks of the four complexes are kept *via* desolvation (Fig. S2, ESI†). The experiment shows the color of the hydrated and dehydrated complex **1** is blue and green, respectively (Fig. S3, ESI†). Immerse the desolvated complex **1** into water and the green solid becomes blue immediately. Whereas immerse in other solvents such as DMF, acetone, tetrahydrofuran, the color of the green solid is unchanged (Fig. S3, ESI†). The PXRD pattern of the re-hydrated sample is similar to the simulated PXRD pattern of complex **1** (Fig. S2(a), ESI†). It is indicated that the solvent water molecules can reversibly enter into the cavities of complex **1**, accompanying with the color change of the sample. No color change is observed in other solvents such as DMF, acetone, tetrahydrofuran, *etc.*, it is probably due to their bigger size than that of water and they can't enter into the cavities of complex **1** freely. The phenomenon is in agreement with our single-crystal data and TG result, it is indicated that only solvent water molecules can locate in the cavities of the complex.

As for complex **2**, the color of the hydrated and dehydrated sample is green and off-white, respectively (Fig. S4, ESI†). More interestingly, when the dehydrated complex **2** is left to stand in an open vessel, the dehydrated off-white sample can absorb the water in air and becomes green quickly. When dried in oven, the color is recovered to be off-white again (Fig. S4, ESI†). The PXRD patterns of the dehydrated and re-hydrated samples are similar to the simulated PXRD pattern of complex **2** (Fig. S2(b), ESI†), indicating water molecules can reversibly enter into the cavities of complex **2**. The obvious color change and the sensitivity to water molecules shows the two complexes, complexes **1** and **2** are good candidates for water indicator. Their stable host frameworks make it feasible to be recycled as water indicator.

As for complex **3**, the color of the solvated and desolvated sample is red and purple, respectively (Fig. S5, ESI†). The PXRD patterns of the solvated and desolvated samples are similar to the simulated PXRD pattern of complex **3** (Fig. S2(c), ESI†), indicating the host framework of complex **3** is stable. However, when immerse the desolvated sample in solvents such as DMF and water, only subtle color changes happen, and no obvious color change can be observed by naked eyes, indicating the color change *via* re-absorption is not pronounced and sensitive, and complex **3** is not a feasible candidate for solvent indicator.

As for complex **4**, the color of the solvated and desolvated sample is the same (white). Though the PXRD patterns of the solvated and desolvated samples are similar to the simulated PXRD pattern of complex **4** (Fig. S2(d), ESI†), indicating the host framework of complex **4** is stable, it is not possible to use the complex to act as solvent indicator.

The UV-Vis spectrum of complex **1** in solid state exhibits a strong reflection peak at 475 nm in the range of 200–800 nm, whereas the reflection peak of the UV-Vis spectrum of the dehydrated sample shifts to 496 nm. Complex **2** and its dehydrated sample display visible radiation with λ_{max} at 481 and 450 nm, respectively. Complex **3** shows an intense reflection peak at 408 nm, a weak shoulder peak at 604 nm and a weak reflection peak at 790 nm. In the UV-Vis spectrum of the desolvated sample, the reflection peaks shift to 416, 630 and 830 nm, respectively. As for complex **4**, no obvious peaks are found in the UV-Vis spectra of the solvated and desolvated samples. The UV-Vis spectra results are agreement with the color changes observed by naked eyes in our experiment.

As described above, complexes **1–3** all show reversible color changes *via* desolvation and salvation, whereas complex **4** doesn't possess the property. What is the origin of the color changes? Recently, Tao's group has reported a metal-complex, Fe(tpa)(NCS)₂ (tpa = tris(2-pyridylmethyl)amine), which exhibits a dramatic color change upon exposure to methanol vapour. The color change is due to the strong H bond interactions between the metal-complex and the solvent.¹⁰ Similarly, as described above, in our work, strong H bond interactions are found between the host frameworks and solvents in the structure of complexes **1–3**. Whereas in complex **4**, no strong solvent-induced H bond is observed. The mechanism of color change is probably based on the solvent-induced H-bonds which change the crystal packing of MOFs and lead to the molecular distortion to some extent,¹⁰ then the energy alteration of the visible d–d transition is expected.²

Conclusion

In conclusion, using L ligand, metal(II) salts and coligand, *m*-H₂BDC, four metal(II)-L complexes have been solvothermally synthesized and structurally characterized by single-crystal X-ray diffraction. Complexes **1** and **2** are isomorphous and exhibit chain-like frameworks. Complex **3** displays a 3D architecture and complex **4** shows a corrugated 2D layer. Complexes **3** and **4** were prepared under similar condition except using different metal salts. The work shows the species of metal salts plays an important role in the structures of coordination polymers. Owing to the flexibility of L ligand, L shows a *cis*-conformation in complexes **1** and **2**, an *intermediate*-conformation in complex **3** and a *trans*-conformation in complex **4**. All the four complexes possess stable host frameworks, and complexes **1–3** show reversible color changes *via* desolvation and solvation. The obvious color change of complexes **1** and **2** *via* dehydration and re-hydration, and the sensitivity and selectivity to water as well as the convenient recycling of the two complexes indicate complexes **1** and **2** are potential good candidates for water indicator. This work shows choosing suitable metal ions and ligands, it is possible to construct stable porous MOFs for solvent indicators.

Financial support from the 973 Program (2006CB932903, 2007CB815303), NSFC (20731005, 20821061, and 20873151), NSF of Fujian Province (E0520003), Key Project from CAS, the Fundamental Research Funds for the Central Universities (No. CDJZR10 22 00 09), Chongqing University Postgraduates' Science and Innovation Fund (No. CDJXS10 22 11 43) and Scientific Research Start-up Foundation of Chongqing University are gratefully acknowledged.

References

- (a) C. Reichardt, *Chem. Rev.*, 1994, **94**, 2319; (b) V. W. Yam, K. M. Wong and N. Zhu, *J. Am. Chem. Soc.*, 2002, **124**, 6506; (c) K. Balakrishnan, A. Datar, T. Naddo, J. Huang, R. Oitker, M. Yen, J. Zhao and L. Zang, *J. Am. Chem. Soc.*, 2006, **128**, 7390; (d) J. C. Nelson, J. G. Saven, J. S. Moore and P. G. Wolynes, *Science*, 1997, **277**, 1793; (e) D. G. Yablou and A. M. Schilowitz, *Appl. Spectrosc.*, 2004, **58**, 843; (f) J. Aimi, Y. Nagamine, A. Tsuda, A. Muranaka, M. Uchiyama and T. Aida, *Angew. Chem., Int. Ed.*, 2008, **47**, 5153.
- (a) R. W. Soukup and K. Sone, *Bull. Chem. Soc. Jpn.*, 1987, **60**, 2286; (b) Y. Fukuda, M. Yasuhira and K. Sone, *Bull. Chem. Soc. Jpn.*, 1985, **58**, 3518; (c) W. Linert, R. F. Jameson and A. Taha, *J. Chem. Soc., Dalton Trans.*, 1993, 3181.
- (a) M. A. Rahman, M. S. Won, N. H. Kwon, J. H. Yoon, D. S. Park and Y. B. Shim, *Anal. Chem.*, 2008, **80**, 5307; (b) P. J. Skrdla, S. S. Saavedra, N. R. Armstrong, S. B. Mendes and N. Peyghambarian, *Anal. Chem.*, 1999, **71**, 1332; (c) B. García, S. Aparicio, R. Alcalde, R. Ruiz, M. J. Dávila and J. M. Leal, *J. Phys. Chem. B*, 2004, **108**, 3024; (d) D. G. Cho, J. H. Kim and J. L. Sessler, *J. Am. Chem. Soc.*, 2008, **130**, 12163.
- (a) O. M. Yaghi, M. O'Keeffe, N. W. Ockwig, H. K. Chae, M. Eddaoudi and J. Kim, *Nature*, 2003, **423**, 705; (b) S. L. James, *Chem. Soc. Rev.*, 2003, **32**, 276; (c) G. Ferey, C. Mellot-Draznieks, C. Serre, F. Millange, J. Dutour, S. Surble and I. Margiolaki, *Science*, 2005, **309**, 2040.
- (a) S. K. Ghosh, B. Sareeya and S. Kitagawa, *Angew. Chem., Int. Ed.*, 2008, **47**, 3403; (b) M. Ohba, W. Kaneko, S. Kitagawa, T. Maeda and M. Mito, *J. Am. Chem. Soc.*, 2008, **130**, 4475; (c) S. K. Ghosh, W. Kaneko, D. Kiriya, M. Ohba and S. Kitagawa, *Angew. Chem., Int. Ed.*, 2008, **47**, 8843; (d) R. Matsuda, R. Kitaura, S. Kitagawa, Y. Kubota, R. V. Belosludov, R. C. Kobayashi, H. Sakamoto, T. Chiba, M. Takata, Y. Kawazoe and Y. Mita, *Nature*, 2005, **436**, 238; (e) S. Kitagawa and R. Matsuda, *Coord. Chem. Rev.*, 2007, **251**, 2490.
- (a) B. L. Chen, Y. Yang, F. Zapata, G. Lin, G. D. Qian and E. B. Lobkovsky, *Adv. Mater.*, 2007, **19**, 1693; (b) Y. Q. Huang, B. Ding, H. B. Song, B. Zhao, P. Ren, P. Cheng, H. G. Wang, D. Z. Liao and S. P. Yan, *Chem. Commun.*, 2006, 4906; (c) M. H. Zeng, X. L. Feng, W. X. Zhang and X. M. Chen, *Dalton Trans.*, 2006, 5294.
- (a) Z. Q. Qin, M. C. Jennings and R. J. Puddephatt, *Chem. Commun.*, 2002, 354; (b) Z. Q. Qin, M. C. Jennings and R. J. Puddephatt, *Inorg. Chem.*, 2003, **42**, 1956; (c) N. L. S. Yue, D. J. Eisler, M. C. Jennings and R. J. Puddephatt, *Inorg. Chem.*, 2004, **43**, 7671; (d) N. Yue, Z. Qin, M. C. Jennings, D. J. Eisler and R. J. Puddephatt, *Inorg. Chem. Commun.*, 2003, **6**, 1269; (e) N. N. Adarsh, D. K. Kumar and P. Dastidar, *CrystEngComm*, 2009, **11**, 796.
- (a) A. L. Spek, *J. Appl. Crystallogr.*, 2003, **36**, 7; (b) X. F. Wang, Y. B. Zhang, H. Huang, J. P. Zhang and X. M. Chen, *Cryst. Growth Des.*, 2008, **8**, 4559.
- A. L. Spek, *Acta Crystallogr., Sect. A: Found. Crystallogr.*, 1990, **46**, C34The free water molecules were removed before the cited solvent accessible volume was calculated by PLATON.
- B. Li, R. J. Wei, J. Tao, R. B. Huang, L. S. Zheng and Z. P. Zheng, *J. Am. Chem. Soc.*, 2010, **132**, 1558.